Special issue, XLVI Extraordinary Congress of Polish Physicists, Warsaw, Poland, October 16–18, 2020

Numerical Simulations of Coulomb Crystallization of Trapped Ions

Ł. Kłosowski* and M. Piwiński

Institute of Physics, Faculty of Physics, Astronomy and Informatics, Nicolaus Copernicus University in Toruń,Grudziądzka 5, 87-100 Toruń, Poland

Doi: 10.12693/APhysPolA.139.261 *e-mail: lklos@fizyka.umk.pl

Ensembles of trapped ions can be studied using numerical simulations, which can provide reliable data on molecular dynamics of ion sets, as well as on geometry of such ensembles in equilibrium state. A numerical model used for such simulations is presented and discussed. This includes various approaches to modeling the trap's potential and cooling mechanisms. Several examples of solutions obtained in such calculations are presented.

topics: ion trapping, numerical simulations, Coulomb crystals

1. Introduction

Trapped ions are a very important tool with numerous applications in atomic physics and related fields [1, 2]. Two most common devices used for such studies are Penning and Paul traps. The former uses the combination of static electric and magnetic fields to confine charged particles in space while the latter uses the combination of static and oscillating electric fields. If a set of ions inside a trap is cooled down to a sufficiently low temperature, it can form the so-called Coulomb crystal. It is a partially ordered 1-, 2- or 3-dimensional structure with particular ions occupying well-defined positions. This way, such ions can be used in precise experiments of various types. A partial, short review on such research was recently published by M. Drewsen [3].

Besides experimental investigations of Coulomb crystals, they can also be studied in numerical simulations. Such calculations in some cases have a considerable advantage over experiments, as they can provide information on ion ensembles' dynamics in a time scale inaccessible experimentally. The molecular dynamics simulations are performed by numerous research groups worldwide as a complement to experiments. In this paper, we present numerical procedures used for such calculations by our group in the National Laboratory FAMO in Toruń.

2. Linear Paul trap

The experiments in Toruń are run using a linear Paul trap, with calcium ions cooled optically in a Doppler scheme [4]. Our goal for the simulation is to provide calculations which reproduce our experimental conditions in the most possibly realistic way.

A linear Paul trap is built of a linear quadrupole, oscillating with radio frequency of the order of 1 MHz. Each electrode of the quadrupole is divided into three segments, allowing to introduce an additional static potential confining a trapped ion's motion along the trap's main axis. The details of the trap's geometry can be found in [5, 6].

2.1. Single trapped ion

The single ion's motion inside such a trap is described with

$$\ddot{\boldsymbol{r}} = \frac{Q}{M}\Big(\boldsymbol{E}_{\mathrm{stat}}(\boldsymbol{r}) + \boldsymbol{E}_0(\boldsymbol{r})\cos(\Omega t)\Big), \tag{1}$$

where $\boldsymbol{r}$ is the ion's position vector, Q is the ion's electric charge, M is the ion's mass, $\boldsymbol{E}_{stat}$ is the static electric field vector, $\boldsymbol{E}_0$ is the oscillating electric field amplitude and Ω is the field's angular frequency.

Both static and dynamic fields can be expressed using multipole expansions of corresponding static and dynamic potentials. In the case of a linear quadrupole trap, pure quadrupoles are a very good approximation. Therefore, (1) can be rewritten as

$$\ddot{x} = \frac{Q}{M}\left(\frac{V_{\mathrm{end}}}{L^2} + \frac{V_0\cos(\Omega t)}{R^2}\right)x, \tag{2}$$

$$\ddot{y} = \frac{Q}{M}\left(\frac{V_{\mathrm{end}}}{L^2} - \frac{V_0\cos(\Omega t)}{R^2}\right)y, \tag{3}$$

$$\ddot{z} = -2\frac{Q}{M}\frac{V_{\mathrm{end}}}{L^2}z, \tag{4}$$

where R and L are the geometrical parameters of the trap, V_{end} is the static voltage used between the segments of the trap's electrodes and V_0 is the amplitude of the voltage used to supply the quadrupole oscillations.

In the case of (2) and (3), they can be written as the Mathieu equations. The solutions are stable for some conditions and have a form of a superposition of two kinds of oscillations. (i) The fast oscillations with the frequency Ω are called the micromotion and (ii) the slower ones, called the macromotion, are described with the effective pseudopotential [1]:

$$V_{\text{eff}}(x,y,z) = \left(-\frac{QV_{\text{end}}}{2ML^2} + \frac{Q^2U_0^2}{8M^2\Omega^2R^2}\right)\left(x^2+y^2\right) + \left(\frac{QV_{\text{end}}}{2ML^2}\right)z^2. \quad (5)$$

The potential is anisotropic, harmonic, providing a trapping minimum in the center of the device. Thus, the approximate equations of motion have the form of

$$\ddot{x} = \frac{Q}{M}\left(\frac{V_{\text{end}}}{L^2} - \frac{QU_0^2}{4M^2\Omega^2R^2}\right)x = -\omega_x^2 x, \quad (6)$$

$$\ddot{y} = \frac{Q}{M}\left(\frac{V_{\text{end}}}{L^2} - \frac{QU_0^2}{4M^2\Omega^2R^2}\right)y = -\omega_y^2 y, \quad (7)$$

$$\ddot{z} = -2\frac{QV_{\text{end}}}{ML^2}z = -\omega_z^2 z. \quad (8)$$

2.2. Set of trapped ions

If more than one ion is trapped, an additional electrostatic interaction between particular ions appears. As they have a non-zero charge and are usually quite well space-separated, a pure Coulomb force is a very good approximation for such interactions. This way, (2)–(4) are modified accordingly

$$\ddot{x}_i = \frac{Q_i}{M_i}\left(\frac{V_{\text{end}}}{L} + \frac{V_0\cos(\Omega t)}{R}\right)x_i + \sum_{k=1,k\neq i}^{N}\frac{Q_iQ_k}{4\pi\varepsilon_0 M_i} \times \frac{(x_i-x_k)}{\left[(x_i-x_k)^2+(y_i-y_k)^2+(z_i-z_k)^2\right]^{3/2}}, \quad (9)$$

$$\ddot{y}_i = \frac{Q_i}{M_i}\left(\frac{V_{\text{end}}}{L} - \frac{V_0\cos(\Omega t)}{R}\right)y_i + \sum_{k=1,k\neq i}^{N}\frac{Q_iQ_k}{4\pi\varepsilon_0 M_i} \times \frac{(y_i-y_k)}{\left[(x_i-x_k)^2+(y_i-y_k)^2+(z_i-z_k)^2\right]^{3/2}}, \quad (10)$$

$$\ddot{z}_i = -2\frac{Q_i}{M_i}\frac{V_{\text{end}}}{L}z_i + \sum_{k=1,k\neq i}^{N}\frac{Q_iQ_k}{4\pi\varepsilon_0 M_i} \times \frac{(z_i-z_k)}{\left[(x_i-x_k)^2+(y_i-y_k)^2+(z_i-z_k)^2\right]^{3/2}}, \quad (11)$$

where i is the particular ion's index and N is the total number of ions. If one decides to use the pseudopotential, the equations of motion will have the form

$$\ddot{x}_i = -\omega_{x_i}^2 x_i + \sum_{k=1,k\neq i}^{N}\frac{Q_iQ_k}{4\pi\varepsilon_0 M_i} \times \frac{(x_i-x_k)}{\left[(x_i-x_k)^2+(y_i-y_k)^2+(z_i-z_k)^2\right]^{3/2}}, \quad (12)$$

$$\ddot{y}_i = -\omega_{y_i}^2 y_i + \sum_{k=1,k\neq i}^{N}\frac{Q_iQ_k}{4\pi\varepsilon_0 M_i} \times \frac{(y_i-y_k)}{\left[(x_i-x_k)^2+(y_i-y_k)^2+(z_i-z_k)^2\right]^{3/2}}, \quad (13)$$

$$\ddot{z}_i = -\omega_{z_i}^2 z_i + \sum_{k=1,k\neq i}^{N}\frac{Q_iQ_k}{4\pi\varepsilon_0 M_i} \times \frac{(z_i-z_k)}{\left[(x_i-x_k)^2+(y_i-y_k)^2+(z_i-z_k)^2\right]^{3/2}}, \quad (14)$$

where eigenfrequencies

$$\omega_{x_i}^2 = -\omega_{y_i}^2 = -\frac{Q_i}{M_i}\left(\frac{V_{\text{end}}}{L^2} - \frac{Q_i}{M_i}\frac{U_0^2}{4\Omega^2R^2}\right), \quad (15)$$

$$\omega_{z_i}^2 = 2\frac{Q_i}{M_i}\frac{V_{\text{end}}}{L^2} \quad (16)$$

can be introduced as parameters to the numerical equations of motion.

3. Doppler cooling

In the experiment, a set of ions is optically cooled in a Doppler scheme [4]. Briefly, it uses a laser beam, slightly red-detuned from strong optical transition in the considered ion. A photon from the laser beam can be absorbed if the ion moves against the laser beam. According to linear momentum conservation, velocity of such an ion will be reduced in such an event by amount

$$\Delta p = \frac{h}{\lambda}, \quad (17)$$

where h is the Planck constant and λ is the wavelength of the used laser light.

The ion emits another photon in spontaneous transition which is, however, distributed over all possible directions (not necessarily isotropic). This means that the recoils from photons emitted in repeating events will average to zero, providing an effective loss of linear momentum and kinetic energy.

If the laser beam propagates along the trap's axis and there is only one ion trapped, such a cooling mechanism will allow only for cooling of one degree of freedom of the ion's motion. In the case of more ions, various degrees of freedom are coupled via the Coulomb interactions, so the Doppler cooling will provide cooling of a full motional state.

If the species cooled is calcium, then the involved quantum states form a Λ system which requires the use of an additional repumping laser [6]. This way, two lasers at 397 nm and 866 nm are necessary. Since the 866 nm P–D transition is much weaker than 397 nm S–P (lifetime 94 ns versus 8 ns) and longer wavelength photons carry less linear momentum than the shorter ones, in the analysis only 397 nm photons are taken into account and 866 nm interactions are neglected.

4. Numerical simulations

The numerical simulations procedure is prepared depending on what information we are interested in and expect. A set of (9)–(11) or (12)–(14) can be numerically solved depending on the needs. To provide the Coulomb crystallization or molecular dynamic of the ions' set, the cooling mechanisms must be introduced to (9)–(14).

4.1. Viscosity cooling mechanisms

A simple commonly used approach is to introduce a non-physical mechanism of viscosity (e.g. the ion trapping experiments are always run in vacuum conditions). Such a non-physical mechanism can be used if the effective potential model is applied. Then, the cooling mechanism modifies (12)–(14) to the following form:

$$\ddot{x}_i = -\omega_{x_i}^2 x_i + \sum_{k=1,k\neq i}^{N} \frac{Q_i Q_k}{4\pi\varepsilon_0 M_i} \times \frac{(x_i - x_k)}{\left[(x_i-x_k)^2+(y_i-y_k)^2+(z_i-z_k)^2\right]^{3/2}} - \mu\dot{x}_i, \tag{18}$$

$$\ddot{y}_i = -\omega_{y_i}^2 y_i + \sum_{k=1,k\neq i}^{N} \frac{Q_i Q_k}{4\pi\varepsilon_0 M_i} \times \frac{(y_i - y_k)}{\left[(x_i-x_k)^2+(y_i-y_k)^2+(z_i-z_k)^2\right]^{3/2}} - \mu\dot{y}_i, \tag{19}$$

$$\ddot{z}_i = -\omega_{z_i}^2 z_i + \sum_{k=1,k\neq i}^{N} \frac{Q_i Q_k}{4\pi\varepsilon_0 M_i} \times \frac{(z_i - z_k)}{\left[(x_i-x_k)^2+(y_i-y_k)^2+(z_i-z_k)^2\right]^{3/2}} - \mu\dot{z}_i, \tag{20}$$

where μ is the viscosity coefficient.

4.2. Numerical procedure

The numerical simulation of N ions is realized by solving $6N$ first order equations obtained from (16)–(18) with selected parameters Q_i, M_i, V_0, V_{end}, Ω and μ.

The used method is one of the types of the Runge–Kutta methods. For our case, we deal with a 4th order procedure with a fixed simulation step size. The step size is chosen to be significantly shorter than periods of oscillations of the ion in trapping potential, usually about 100 times shorter. The initial states of ions are chosen randomly, usually in the range of the expected size of an ion ensemble at equilibrium and at room temperature.

Although such an approach provides reliable data on the structure of the ion set in equilibrium, it gives an unrealistic picture of molecular dynamics. It also does not provide information on ions' micromotion. However, the advantage of this approach is high efficiency — the calculation step can be longer than the micromotion oscillation period which means that less calculation steps are required to reach the equilibrium.

4.3. Optical cooling mechanism

A more sophisticated but less effective approach is to simulate momentum transfer in photon absorption from the laser beam. In such a case, simulations are run solving (9)–(11) by using the Runge–Kutta method with a step size much shorter (≈ 1000 times) than the micromotion oscillation period. For example, at $\Omega = 2\pi \times 1$ MHz, the step size is $\Delta t = 1$ ns. At each step, a stochastic action of ion–photon interaction is randomized separately for every ion in the set, with probability p depending on the assumed intensity of the cooling laser beam.

If the interaction is drawn to be true, a following amendment to the ion's velocity vector is made:

- Firstly, one checks whether an ion is in a proper velocity class. Only some class of ions can interact with photons due to atomic transition's natural width and the Doppler shifting. For example, at cooling of calcium ions (mass 40 amu), a 397 nm transition of 8 ns lifetime is used. For simplicity, less probable 866 nm transitions are not taken into account. The width of the ion velocity class sensitive to photons is then

$$\Delta v = \frac{397 \text{ nm}}{8 \text{ ns}} \approx 50 \frac{\text{m}}{\text{s}}. \tag{21}$$

- If the value of the z component is below Δv, then only in such a case the amendment procedure is continued. Effectively, this means that we assume the rectangular shape of a natural transition line. The applied approximation allows then to avoid a more complex line shape modeling.

- If the ion is found to be a subject to optical interaction, then two changes to the velocity vector are realized: one connected with absorption of a photon from the laser beam and one from fluorescence. Since the fluorescence direction is random, the direction of momentum transfer must be randomized in the numerical procedure. In a real situation, the distribution of such fluorescence is determined by the polarization of the laser beam and the presence of magnetic field due to the Hanle effect [7]. In the simulations, the isotropic distribution is assumed for simplicity. If we assure this, then two numbers p_1 and p_2 must be drawn from rectangular distribution ranging from $(0, 1)$. The random amendments to velocity components are then calculated using

$$\delta\dot{x} = \frac{2h}{\lambda M}\sqrt{p_1(1-p_1)}\cos(2\pi p_2), \tag{22}$$

$$\delta\dot{y} = \frac{2h}{\lambda M}\sqrt{p_1(1-p_1)}\sin(2\pi p_2), \tag{23}$$

$$\delta\dot{z} = -\frac{2h}{\lambda M} p_1, \tag{24}$$

where the maximum velocity transfer is $\frac{2h}{\lambda M} \approx 0.05\ \frac{\mathrm{m}}{\mathrm{s}}$.

The procedure simulating the ion–photon interaction can be further repeated for photons coming from different directions, for example to simulate more laser beams.

5. Results and summary

The simulations described above can be run in various conditions, i.e., involving a number of ions, their masses and charges (they may vary in the set), a number of ions susceptible to cooling, trapping potential shapes, depths, and frequencies. Due to a large variety of possibilities, only several simple examples were selected to be presented here.

The simulations were run of an ensemble of 40 ions being cooled in three different ways: a weak optical beam, a strong optical beam and using the approximation of effective potential and viscosity cooling. Examples of trajectories of ions are presented in Fig. 1. Obtained equilibrium states are presented in Figs. 2–4. All the calculations were performed with conditions corresponding to typical experimental conditions of $\Omega = 2\pi \times 6$ MHz, $V_0 = 800$ V and $V_{\mathrm{end}} = 15$ V.

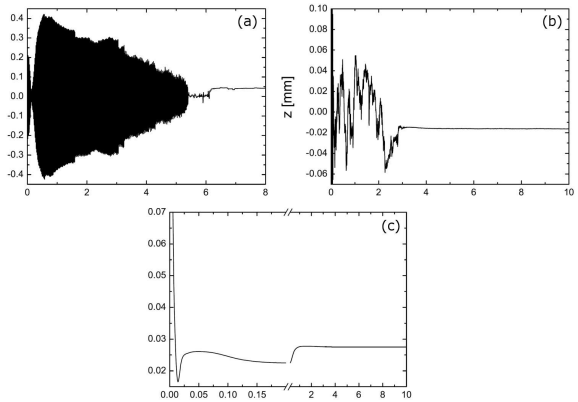

Fig. 1. Examples of dynamics of a trapped ion while being cooled. Part (a) represents weak optical cooling (average interval 50 ns between photon collisions). Part (b) represents strong optical cooling (5 ns between collisions). Part (c) is a viscous cooling result. All three graphs represent the z position of one, randomly selected ion from the ensemble of 40. It is clear that the viscous cooling is more effective than the optical one. A stronger optical beam allows to reach equilibrium in a shorter time. There are some ion jumps visible for an already cooled ion in a strong field. They can be interpreted as a result of slower cooling of x and y degrees of freedom which are not presented in the graph.

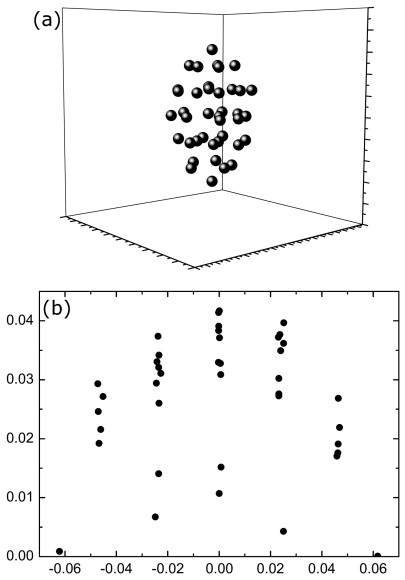

Fig. 2. A Coulomb crystal obtained in strong optical cooling. Part (a) is a 3-dimensional picture. Part (b) is a projection of the ions' position along an azimuthal coordinate. A "string of disks" structure is clearly visible in the crystal's geometry.

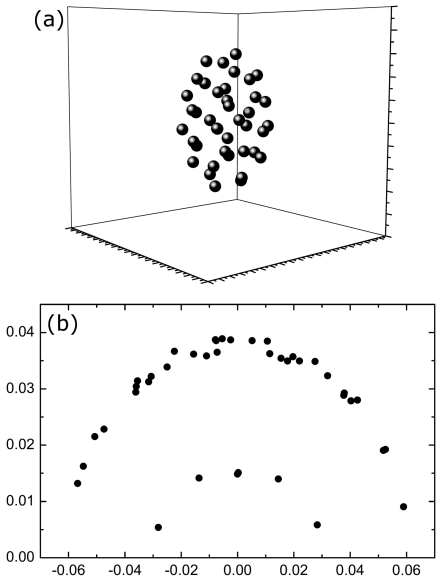

Fig. 3. A Coulomb crystal obtained in viscous cooling. Part (a) is a 3-dimensional picture. Part (b) is a projection of the ions' position along an azimuthal coordinate. A spheroidal shell structure (two shells in this case) is visible in the crystal's geometry.

In all three cases, the ions formed the Coulomb crystals, however, their dynamics were different. The equilibrium state was achieved in a much shorter time for viscous cooling than for the optical one. Also, the cooling with a stronger optical beam intensity ensures quicker achieving of the equilibrium.

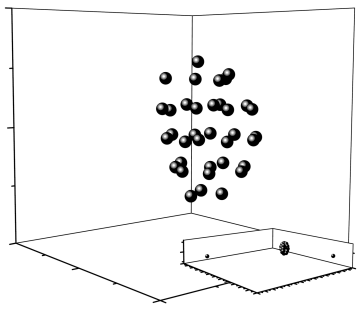

Fig. 4. A Coulomb crystal obtained in weak optical cooling. The inset in the bottom right-hand corner is a zoomed-out view of the crystal. It can be noticed that two of the ions are not included in the crystal and instead they are orbiting it in the xy plane.

In the case of viscous cooling, the ions formed a typically observed shell structure. To improve visibility of such a geometry, we present an azimuthal projection of the formed crystal in Figs. 2 and 3.

In the case of optical cooling, the ions were arranged in a "string of disks" structure — similar to the one observed in some experiments [8]. This effect may be interpreted as a result of strong optical confinement of ions along one of the degrees of freedom (the z axis in this case). This, in fact, will be the subject of our further theoretical investigations with various directions and number of laser beams.

At weaker optical cooling, in some cases "satellite ions" remain outside the formed Coulomb crystal. An example of such ions is presented in Fig. 4. The mechanism of the particles appearance is based on the cooling efficiency in z direction only. If an ion is sufficiently far from the trap's center, its x, y degrees of freedom are weakly coupled via the Coulomb interaction with z. Hence, such "satellites" effect is typically observed in experiment for the Coulomb crystal trapping. It can be seen for many seconds, until these ions are knocked down for example in a collision with background gas.

6. Conclusions

There are several possible approaches to simulate the behavior of sets of trapped ions. Some of them, such as the model presented in this paper, provide more realistic solutions but are more time-consuming. Others, such as the one using effective potentials or a viscous mechanism of cooling, are much more time-efficient in obtaining equilibrium, however, they provide a less realistic mechanism of equilibration.

The presented models of ion cooling are applicable for certain experimental cases only. The viscous one can be used whenever vacuum and temperature conditions are sufficient for the Coulomb crystallization. Also, a low micromotion amplitude (much below the distance between ions in a crystal) is required to provide a good comparison between calculations and experiment. The simulation results will indeed reproduce the geometry of ion ensembles in equilibrium, however, the dynamics of equilibration will not be well-reproduced.

The optical cooling model is applicable when the cooling beam geometry is well-defined and interactions such as ion–background gas collisions are negligible. Performing a model including such interactions will be the subject of our future studies.

References

[1] F.G. Major, V.N. Gheorghe, G. Werth, *Charged Particle Traps, Physics and Techniques of Charged Particle Field Confinement*, Springer, 2005.

[2] G. Werth, V.N. Gheorghe, F.G. Major, *Charged Particle Traps II, Applications*, Springer, 2009.

[3] M. Drewsen, *Physica B Condens. Matter* **460**, 105 (2015).

[4] S. Stenholm, *Rev. Mod. Phys.* **58**, 699 (1986).

[5] Ł. Kłosowski, M. Piwiński, K. Pleskacz, S. Wójtewicz, D. Lisak, *J. Mass Spectrom.* **53**, 541 (2018).

[6] Ł. Kłosowski, K. Pleskacz, S. Wójtewicz, D. Lisak, M. Piwiński, *Photon. Lett. Poland* **9**, 119 (2017).

[7] Ł. Kłosowski, M. Piwiński, D. Dziczek, K. Wiśniewska, S. Chwirot, *Meas. Sci. Technol.* **18**, 3801 (2007).

[8] N. Kjærgaard, M. Drewsen, *Phys. Rev. Lett.* **91**, 095002 (2003).